ARTICLE

The thermoacidophilic methanotroph *Methylacidiphilum fumariolicum* SolV oxidizes subatmospheric H_2 with a high-affinity, membrane-associated [NiFe] hydrogenase

Rob A. Schmitz [1] · Arjan Pol[1] · Sepehr S. Mohammadi[1] · Carmen Hogendoorn[1] · Antonie H. van Gelder[2] ·
Mike S. M. Jetten [1] · Lena J. Daumann [3] · Huub J. M. Op den Camp [1]

Abstract

The trace amounts (0.53 ppmv) of atmospheric hydrogen gas (H_2) can be utilized by microorganisms to persist during dormancy. This process is catalyzed by certain Actinobacteria, Acidobacteria, and Chloroflexi, and is estimated to convert 75×10^{12} g H_2 annually, which is half of the total atmospheric H_2. This rapid atmospheric H_2 turnover is hypothesized to be catalyzed by high-affinity [NiFe] hydrogenases. However, apparent high-affinity H_2 oxidation has only been shown in whole cells, rather than for the purified enzyme. Here, we show that the membrane-associated hydrogenase from the thermoacidophilic methanotroph *Methylacidiphilum fumariolicum* SolV possesses a high apparent affinity ($K_{m(app)} = 140$ nM) for H_2 and that methanotrophs can oxidize subatmospheric H_2. Our findings add to the evidence that the group 1h [NiFe] hydrogenase is accountable for atmospheric H_2 oxidation and that it therefore could be a strong controlling factor in the global H_2 cycle. We show that the isolated enzyme possesses a lower affinity ($K_m = 300$ nM) for H_2 than the membrane-associated enzyme. Hence, the membrane association seems essential for a high affinity for H_2. The enzyme is extremely thermostable and remains folded up to 95 °C. Strain SolV is the only known organism in which the group 1h [NiFe] hydrogenase is responsible for rapid growth on H_2 as sole energy source as well as oxidation of subatmospheric H_2. The ability to conserve energy from H_2 could increase fitness of verrucomicrobial methanotrophs in geothermal ecosystems with varying CH_4 fluxes. We propose that H_2 oxidation can enhance growth of methanotrophs in aerated methane-driven ecosystems. Group 1h [NiFe] hydrogenases could therefore contribute to mitigation of global warming, since CH_4 is an important and extremely potent greenhouse gas.

Introduction

Hydrogen gas (H_2) is thought to be the first available energy source on early Earth and is still ubiquitously used by a plethora of microorganisms [1, 2]. Hydrogenases convert H_2 into two protons or vice versa and are classified based on the metals within the interior of the active site: either [NiFe], [FeFe], or [Fe] [3]. Low-affinity H_2 oxidation is catalyzed by microbes in habitats with relatively high H_2 availability, e.g., animal guts and leguminous soils [4, 5]. On the contrary, high-affinity microorganisms can oxidize atmospheric H_2 (0.53 ppmv H_2) [6]. Soils constitute the largest sink, consuming ~75% of the total atmospheric H_2, resulting in an atmospheric turnover rate of 75 Tg H_2 per year [6–8]. Several Actinobacteria isolated from soils are able to oxidize atmospheric H_2 [9–11]. They have an apparent high affinity ($K_{m(app)} \sim 10$–400 nM H_2) for H_2. All these high-affinity actinobacterial isolates encode for the novel group 1h [NiFe] hydrogenase (Hyd-1h). This genetic finding led to the hypothesis that atmospheric H_2 is oxidized by this type of hydrogenase in particular [10, 11]. However, microorganisms encoding the group 2a or group 1f [NiFe]

✉ Huub J. M. Op den Camp
h.opdencamp@science.ru.nl

1 Department of Microbiology, Radboud University, Heyendaalseweg 135, NL-6525 AJ Nijmegen, The Netherlands

2 Laboratory of Microbiology, Wageningen University and Research, Stippeneng 4, 6708 WE Wageningen, The Netherlands

3 Department Chemie, Ludwig-Maximilians-Universität München, Butenandtstraβe 5-13, D-81377 München, Germany

hydrogenase were also shown to mediate atmospheric H_2 oxidation [12, 13]. Nevertheless, currently it is unknown whether these hydrogenases possess an intrinsic high affinity for H_2, or whether other cellular factors such as the respiratory chain modulate their affinity [12]. The betaproteobacterium *Ralstonia eutropha* H16 encodes for a group 1h [NiFe] hydrogenase, but this strain is unable to oxidize atmospheric H_2 [14]. Indeed, purification of this putative high-affinity hydrogenase revealed a relatively high K_m value of 3.6 μM, reflecting a low affinity [14]. Other studies have only investigated atmospheric H_2 oxidation in whole cells [9, 10, 15–20]. Hence, the question remains whether Hyd-1h from an organism capable of atmospheric H_2 oxidation will show a high affinity for H_2 after purification.

Although group 1h [NiFe] hydrogenases are predominantly encoded by Actinobacteria, examples in other phyla exist [12]. Atmospheric H_2 oxidation has been observed in Actinobacteria, Acidobacteria, and Chloroflexi [12, 15, 18]. In addition, a conserved group 1h [NiFe] hydrogenase orthologue is highly expressed in the mud volcano-inhabiting methanotroph *Methylacidiphilum fumariolicum* SolV of the Verrucomicrobia phylum [21, 22]. Verrucomicrobia are dominant bacteria in (volcanic) soils and geothermal habitats [23, 24]. Verrucomicrobial methanotrophs are autotrophs that fix CO_2 via the Calvin–Benson–Bassham cycle [25]. *M. fumariolicum* SolV can grow below pH 1 and is dependent on certain rare-earth elements (early lanthanides) for growth [26]. Remarkably, the Hyd-1h enables this bacterium to grow rapidly on H_2 as sole energy source, which is in contrast to previously reported high-affinity isolates, in which the Hyd-1h is utilized during starvation to persist on atmospheric H_2 [16, 27, 28]. The ability of methanotrophs to consume H_2 as additional energy source provides a major advantage in ecosystems where CH_4 availability fluctuates [29]. Previously, mixotrophy was proven to drive niche expansion of verrucomicrobial methanotrophs [30]. Methanotrophs mitigate greenhouse gas emissions from geothermal areas, which could be enhanced by hydrogenases. However, it is unknown whether methanotrophs or Verrucomicrobia are also able to oxidize atmospheric H_2. Numerous studies have focused on the physiology of atmospheric H_2 scavenging during dormancy [10, 11, 14, 27], but biochemical studies on the putative high-affinity Hyd-1h are scarce. Interestingly, the membrane association of the Hyd-1h seems to be essential for high-affinity atmospheric H_2 oxidation [12, 14, 15, 27, 31]. Indeed, the cytoplasmic Hyd-1h from *R. eutropha* H16 is a low-affinity enzyme, whereas whole cell studies in microbes with membrane-associated Hyd-1h show the contrary [12, 18]. In this study, we show that methanotrophs can oxidize atmospheric H_2, using the membrane-associated group 1h [NiFe] hydrogenase. Remarkably, the Hyd-1h of the verrucomicrobial

methanotroph studied here not only enables strain SolV to oxidize atmospheric H_2, but also to rapidly grow on geothermally derived H_2 [22]. However, we could not show that the isolated enzyme is able to oxidize atmospheric H_2. The isolated enzyme possesses a lower affinity for H_2 compared with the apparent high affinity of the enzyme in association with the membrane, indicating that the membrane association is pivotal to the ability to oxidize atmospheric H_2. We propose that the Hyd-1h provides *M. fumariolicum* SolV a survival benefit that could therefore enhance mitigation of CH_4 emissions from methanotrophic ecosystems.

Materials and methods

Strain and growth conditions

Methylacidiphilum fumariolicum SolV cells were grown as pure culture in a 7 L bioreactor controlled by in-Control (Applikon, Delft, The Netherlands) with a working volume of 5 L. The growth medium was composed of 0.2 mM $MgCl_2 \cdot H_2O$, 0.2 mM $CaCl_2 \cdot H_2O$, 1 mM Na_2SO_4, 2 mM K_2SO_4, 2 mM $(NH_4)_2SO_4$, and 50 μM $NaH_2PO_4 \cdot H_2O$. The final trace element concentration was 1 μM $NiCl_2 \cdot 6H_2O$, $CoCl_2 \cdot 6H_2O$, $NaMoO_4 \cdot 2H_2O$, and $ZnSO_4 \cdot 7H_2O$, 5 μM $MnCl_2 \cdot 4H_2O$ and $FeSO_4 \cdot 7H_2O$, 10 μM $CuSO_4 \cdot 5H_2O$, and 20 nM $CeCl_3 \cdot 6H_2O$. The temperature was 55 °C and maintained using a heat blanket. The pH was measured by a pH electrode and controlled at 3.0 by automatic addition of 1 M NaOH. The dissolved oxygen (DO) concentration was measured by an oxygen electrode. The airflow was regulated to maintain a DO concentration of 1% air saturation. The reactor was stirred at 500 rpm using a stirrer with two Rushton impellers. The reactor was supplied with 70 mL min^{-1} CO_2–Ar (5%:95% (v/v)), 10 mL min^{-1} CH_4–CO_2 (95%:5% (v/v)) and 6 mL min^{-1} H_2.

Cells (and membranes) used to investigate atmospheric H_2 oxidation and kinetics were gained from a culture grown on H_2 limitation. Cells in the 0.5 L bioreactor (Applikon) were supplied with a mixture of argon, H_2 (0.7% (v/v)), and CO_2 (10% (v/v)) at 5 mL min^{-1}. Five millimolars $NaNO_3$ was used as nitrogen source instead of ammonium. The DO concentration was kept between 0.2 and 1% O_2 saturation.

Gas chromatography

Atmospheric H_2 was measured on a CompactGC (Global Analyser Solutions, Breda, The Netherlands) with a pulsed discharge ionization detector with an input range of 8 nA. One hundred twenty milliliters serum bottles containing 10 mL cell suspension ($OD_{600} = 0.12$) were used, capped with a rubber stopper. The heat-killed control was

autoclaved at 121 °C for 15 min. The bottles were made anoxic by flushing with N_2, after which 1 mL O_2 and 3 mL CO_2 were added to the headspace. H_2 was added from a stock diluted in N_2 to obtain trace concentrations. To test whether the purified Hyd-1h could oxidize atmospheric H_2, 120 serum bottles were filled with 5 mL 50 mM KP_i (pH 7.0), 500 µM nitroblue tetrazolium. 0.3 mg mL^{-1} bovine serum albumin was present in the bottles to create a stable protein environment. The bottles were made anoxic by flushing with N_2. The assay was initiated by addition of 30 µg purified hydrogenase. Bottles containing cells or pure enzyme were incubated at 55 and 40 °C, respectively, at 300 rpm. Biological triplicates were used and for each data point 0.2 mL headspace was sampled.

Preparation of cell fractions and enzyme purification

Cells were harvested by centrifugation (15 min, $5000 \times g$, 4 °C), resuspended in 20 mM bis-Tris buffer (pH 7.0), and passed through a French pressure cell (120 MPa, three times; American Instrument Company, Silver Spring, MD, USA). Hereafter, the crude extract (CE) was obtained by collecting the supernatant after centrifugation (10 min, $10,000 \times g$, 4 °C). Subsequently, the CE was centrifuged (1 h, $137,000 \times g$, 4 °C). The pellet, containing the membrane proteins and membranes (membrane fraction; MF), was homogenized using a 15 mL Potter-Elvehjem tissue grinder (DWK Life Sciences, Mainz, Germany) and subsequently mixed with 1% (v/v) n-dodecyl-β-maltoside for 1 h at room temperature (RT) by gentle stirring. This suspension was centrifuged again (1 h, $137,000 \times g$, 4 °C). The supernatant containing the solubilized MF (SMF) was used for protein purification, carried out aerobically at RT on an Äktapurifier (GE Healthcare Bio-Science AB, Uppsala, Sweden). All buffers contained 0.02% (v/v) n-dodecyl-β-maltoside. Hyd-1h was purified using three different consecutive columns. First, the SMF was loaded onto a prepacked Q Sepharose column (GE Healthcare, Chicago, IL, USA), equilibrated with 20 mM bis-Tris (pH 7.0). Then, the sample was loaded and the column was washed with 20 mM bis-Tris 100 mM NaCl (pH 7.0). Hereafter, the column was washed with 20 mM bis-Tris 200 mM NaCl (pH 7.0) and the most active fractions were pooled. Subsequently, the buffer of the sample was exchanged to 20 mM KP_i (pH 7.0) and the concentrated sample was loaded onto a prepacked CHT ceramic hydroxyapatite column (Bio-Rad, Hercules, CA, USA), equilibrated with 20 mM KP_i (pH 7.0). Hereafter, a gradient of 30 column volumes to 500 mM KP_i (pH 7.0) was performed. The most active fractions were pooled and the buffer of the sample was exchanged back to 20 mM bis-Tris (pH 7.0). Finally, the sample was loaded onto a prepacked TSKgel DEAE-5PW column

(Merck, Darmstadt, Germany), equilibrated with 20 mM bis-Tris (pH 7.0). The hydrogenase was eluted during a gradient of 20 column volumes to 20 mM bis-Tris 300 mM NaCl (pH 7.0). The purified enzyme (in 20 mM bis-Tris buffer, 200 mM NaCl, 0.02% (v/v) n-dodecyl-β-maltoside, pH 7.0) was snap-frozen in liquid nitrogen and stored at −80 °C. Protein concentrations of the different samples were measured using the BCA method (Thermo Fisher Scientific, Waltham, MA, USA) with bovine serum albumin as standards.

Kinetic studies using membrane-inlet mass spectrometry (MIMS)

Liquid concentrations of H_2 were measured by MIMS (HPR40, positive ion counting detector, Hiden Analytical, Warrington, UK) in a 10 mL chamber (Fig. S3). The MIMS probe was inserted inside of the bottom part just above the glass stirrer bar (1000 rpm). The probe was mounted with a 10 µm thin silicon (Hiden Analytical) or PTFE (Hansatech, Pentney, UK) membrane (8 mm^2). The liquid was equilibrated with the desired gas by bubbling the gas into the liquid via a metal capillary inserted via the central hole in the piston. When equilibrated, the capillary was removed and the piston was lowered until the liquid filled up the central hole (0.8 mm diameter) and ensuring no gas bubbles were trapped inside the chamber. The liquid volume was between 8 and 9 mL. All additions were done via the same hole by gastight syringes (Hamilton, Reno, NV, USA). Signals of mass 2 were not only from H_2 but resulted also from water and gases such as CO_2. Therefore, the vacuum line (1/8 in. stainless steel tubing) connecting the membrane probe with the mass spectrometer had a coiled part (three windings of 8 cm diameter) inserted in liquid nitrogen to trap water vapor and other gases that pass the silicon membrane. In this way, the background mass 2 signal was minimized. For maximum sensitivity, the electron emission current was optimized at 400 µA. For calibrations, known amounts of gas-saturated water were administered from 50 mL serum bottles containing 10 mL water. The headspaces were exchanged and pressurized with pure gas at 1–1.3 bar and stoppered by butyl rubber stoppers. For water, a solubility of 807 µM at RT was used [32]. For O_2, a solubility of 1.35 mM at atmospheric pressure was used. In the experiment with whole cells, the medium used was identical to the growth medium and the pH value was as during growth. In the experiment with membranes, 20 mM bis-Tris buffer (pH 7.0) was used. The initial DO concentration was set at 1% by bubbling with a mixture of argon, CO_2 (5%), and O_2 (1%). During respiration of H_2, the O_2 concentration was maintained between 0.5 and 1% DO by adding O_2-saturated medium. Either cells from the chemostat or the MF were used at 50 and 40 °C,

respectively. With the MF, either 110 μM methylene blue (MB) or 100 μM Wurster's blue (WB) was used as electron acceptor. When working with the isolated enzyme, 100 μM nitroblue tetrazolium was used as electron acceptor. The cell was thoroughly flushed with argon and 0.3 mg mL^{-1} bovine serum albumin was supplemented to stabilize the 250 ng isolated enzyme used in the experiment. After the data were gathered, the curve was fitted according Michaelis–Menten kinetics. From this fit, the maximum oxidation rates (V_{max}) and (apparent) affinity constants (K_m) could be determined.

Gel electrophoresis and mass spectrometry

SDS-polyacrylamide gels for molecular mass determination of the proteins were made and run as described by [33]. Five microliters PageRuler Plus Prestained Protein Ladder (Thermo Fisher Scientific) was used as molecular ladder. To identify bands on the SDS-polyacrylamide gels, samples were analyzed with the use of matrix-assisted laser desorption/ionization time-of-flight mass spectrometry. Therefore, samples were prepared and analyzed as described by [33]. A calibrant protein mixture was prepared from 10 pmol stocks by mixing 1 μL adrenocorticotropic hormone, 1.5 μL synthetic peptide P14R, 2 μL bradykinin, 2 μL angiotensin II, and 6.5 μL 4-hydroxy-α-cyanocinnamic acid matrix. One microliter of this mixture was used for analysis. Gene identifiers in the text refer to the Genoscope Platform. The GenBank identifiers for the large and small subunit of Hyd-1h are MFUMSOLV_RS08465 and MFUM-SOLV_RS08470, respectively.

Spectrophotometric enzyme assays

Activity assays were performed in 1.4 mL 10.00 mm quartz cuvettes at 50 °C and initiated by addition of the protein sample or cell fraction. The cuvettes were filled with H$_2$-saturated 20 mM bis-Tris (pH 7.0) and 1 mM nitroblue tetrazolium and immediately closed with a plastic cap at RT. A small headspace with ambient air was always present. Cuvettes containing buffer were preincubated for 5 min at the right temperature at which the experiment would take place, while the background signal was measured. Reduction of nitroblue tetrazolium was followed at 593 nm. The thermostability assay was performed at 50 °C with purified enzyme preincubated at 70, 80, and 85 °C for 30 min. The temperature optimum experiment was measured from 30 to 100 °C with increments of 10 °C. The pH optimum experiment was measured from pH 4 to 10 in a Britton–Robinson pH system at 50 °C containing 40 mM phosphoric acid, boric acid, and acetic acid [34]. In spectrophotometry assays, initial rates in the first 30 s were used to determine the H$_2$ oxidation rates.

Circular dichroism

The J-810 circular dichroism spectrometer (Jasco, Oklahoma City, USA) was used to observe changes in secondary structure upon temperature change. A scanning speed of 100 nm min^{-1}, a data pitch of 0.1 nm, a data integration time of 1 s, and a bandwidth of 1.0 nm were used. Baseline spectra of the buffer at different temperatures were recorded and subtracted from the protein spectrum at the corresponding temperature. Spectra were obtained from 200 to 260 nm, measured after 1, 30, and 60 min incubation at 95 °C. The buffer of the sample was exchanged to 20 mM phosphate buffer (pH 7.0) to reduce background signal.

Results

M. fumariolicum SolV oxidizes subatmospheric H$_2$ with apparent high affinity

M. fumariolicum SolV cells incubated at 55 °C oxidized 29 ± 1.3 ppmv H$_2$ to well below the atmospheric H$_2$ threshold within 18 h (Fig. 1). A second addition of H$_2$ after 29 h again resulted in the rapid first-order oxidation of H$_2$ (3.15 ± 0.32 ppmv H$_2$ h^{-1}) below the atmospheric H$_2$ threshold. Heat-killed cells did not show any H$_2$ uptake, confirming the process to be biotic. Kinetic parameters of H$_2$ consumption were determined in a closed cell with a diluted culture and no gas phase by measuring H$_2$ with MIMS. This technique was conducted to avoid mass transfer problems and the limitation in sampling
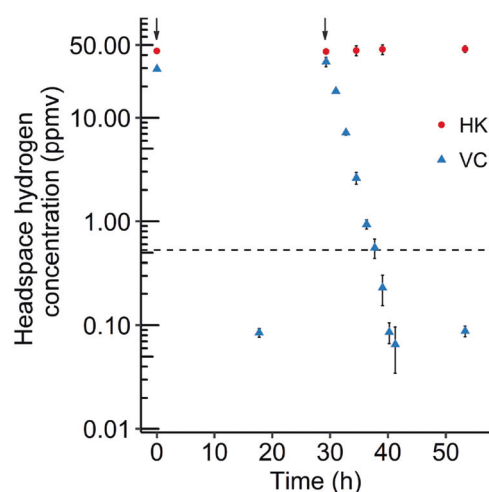

Fig. 1 **Subatmospheric H$_2$ oxidation by Hyd-1h in cells of *Methylacidiphilum fumariolicum* SolV.** The dashed line indicates the atmospheric H$_2$ concentration (0.53 ppmv). The arrows indicate when hydrogen gas was added. One hundred twenty milliliters capped serum bottles were inoculated with 10 mL (OD$_{600}$ = 0.12) heat-killed cells (HK) or viable cells (VC). At 29 h, H$_2$ was again supplemented to VC. Error bars indicate standard deviations ($n = 3$).
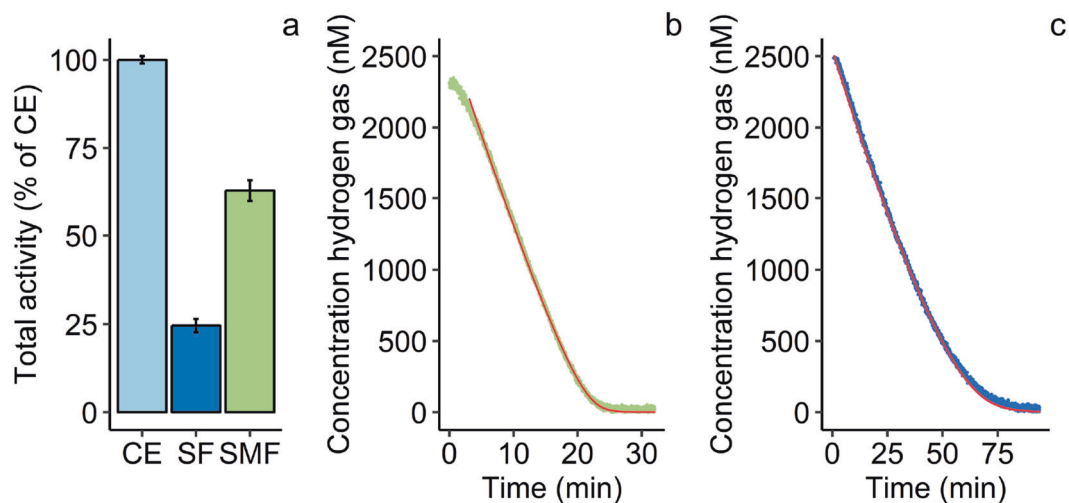
Fig. 2 H$_2$ oxidation by Hyd-1h. a Total H$_2$-oxidizing activity of the soluble fraction (SF) and the solubilized membrane fraction (SMF) in % of the total activity of crude extract (CE). Activity was measured spectrophotometrically at 593 nm at 50 °C as reduction of the electron acceptor nitroblue tetrazolium. Error bars indicate standard deviations ($n = 3$). **b** High-affinity H$_2$ oxidation by the membrane-associated Hyd-1h with methylene blue as electron acceptor. **c** H$_2$ oxidation by the purified Hyd-1h with nitroblue tetrazolium as electron acceptor. Hydrogen gas was measured at 40 °C by the membrane-inlet mass spectrometer (MIMS). To determine kinetic parameters, data points were fitted according to Michaelis–Menten kinetics. The red lines show the fitted curves.

encountered with headspace measurements for gas chromatography. The maximum H$_2$ oxidation rate ($V_{\text{max(app)}}$) was measured to be 340 nmol H$_2$ min^{-1} mg DW^{-1} and the cells have an apparent high affinity ($K_{\text{m(app)}}$) for H$_2$ of 195 ± 10 nM ($n = 8$; Fig. S1). To ensure that only Hyd-1h was responsible for the observed H$_2$ consumption down to the threshold level of the MIMS (20 nM), the cells used were cultivated in a chemostat under such conditions that only Hyd-1h (MfumV2_0978-9) was expressed, but not the oxygen-sensitive group 1d [NiFe] hydrogenase (MfumV2_1564-5) [22]. Similarly, experiments were performed in the presence of at least 0.2% O$_2$, so that traces of the group 1d [NiFe] hydrogenase would be inactive [22]. The apparent kinetic parameters strongly suggest that Hyd-1h is solely accountable for subatmospheric H$_2$ oxidation in the methanotroph *M. fumariolicum* SolV.

Membrane-associated Hyd-1h possesses an apparent high affinity for H$_2$

Analysis of the two genes (MfumV2_0978-9) encoding Hyd-1h revealed no transmembrane helices nor a signal peptide, suggesting that the enzyme resides within the cytoplasm without membrane anchor [35, 36]. Nevertheless, the total activity measured in the SMF exceeds that of the soluble fraction (SF) more than 2.5-fold (Fig. 2a). This membrane association could enable energy conservation and could be formed through a currently unknown physiological redox partner protein [37]. The activity of the SF could be a combination of Hyd-1h and the putative NADH-reducing group 3b [NiFe] hydrogenase (MfumV2_2420-1; [30]).

However, expression of Hyd-1h is 20–40-fold higher compared with the expression of the group 3b [NiFe] hydrogenase at various conditions [22]. In addition, strain SolV was grown at such an O$_2$ concentration that the group 1d [NiFe] hydrogenase is barely expressed [22]. Therefore, the activity of the CE can be primarily attributed to Hyd-1h. The enzyme is bound weakly to the membrane so that the activity is found in both SF and SMF.

The group 1h [NiFe] hydrogenase mediates atmospheric H$_2$ oxidation, but it is still unknown whether the isolated enzyme has a high affinity for H$_2$ or that this affinity is modulated by other cellular factors [12, 18, 22]. Since the enzyme tends to associate with the membrane, which seems to be important for enzyme functioning, kinetics would be most accurately determined by mimicking these conditions [14]. To determine kinetic parameters of the membrane-associated hydrogenase only, the enzyme needed to be decoupled from the remainder of the electron transport chain. For this purpose, membranes of strain SolV were isolated and MB (redox potential = +10 mV) was used as electron acceptor [27]. As a consequence, electrons released by Hyd-1h would be taken up before flowing to electron transport chain proteins with a higher redox potential (e.g., complex III and the terminal oxidase). When enzyme kinetics were assayed with MIMS, we could show that the membrane-associated Hyd-1h possesses a high apparent affinity ($K_{\text{m(app)}}$) of 140 ± 10 nM ($n = 4$) and a maximum velocity ($V_{\text{max(app)}}$) of 38 nmol H$_2$ min^{-1} mg protein^{-1} (Fig. 2b). Furthermore, WB (redox potential = + 276 mV) was used as electron acceptor. When WB was used, a significantly higher affinity of 90 ± 5 nM ($n = 4$) was

determined. However, the maximum velocity decreased severely after subsequent H_2 additions after H_2 depletion (from 67 to 37 nmol H_2 min^{-1} mg protein^{-1}). On the contrary, maximum rates did not decrease over time when MB was used as electron acceptor. Apparently, different artificial electron acceptors reveal different kinetic parameters. The parameters of the membrane-associated Hyd-1h were most stably determined with MB as electron acceptor.

Hyd-1h purified from native biomass is highly thermostable

To investigate enzyme characteristics such as thermostability, the enzyme needs to be devoid of other proteins that could interfere. Therefore, the enzyme was purified 45-fold from the SMF to a specific activity of 18.4 μmol H_2 min^{-1} mg protein^{-1} (Table S1). The specific activity of the SMF is more than twice as high as the specific activity of the CE. Hence, Hyd-1h was purified approximately 100-fold from the CE. Two bands with apparent sizes of 65 and 40 kDa could be observed on a denaturing SDS-polyacrylamide gel after purification (Fig. S2). The large and small band were identified with matrix-assisted laser desorption/ionization mass spectrometry as the large (HhyL; MfumV2_0979) and small (HhyS; MfumV2_0978) subunit of Hyd-1h, respectively. Whereas cells of strain SolV are able to oxidize 30 ppmv H_2 to well below the atmospheric H_2 threshold, the purified enzyme was unable to do so. The activity of the isolated enzyme diminishes over time, which could be largely overcome by using a concentration of 0.3 mg mL^{-1} bovine serum albumin to create a stabilizing protein environment. The affinity for H_2 of the isolated enzyme was determined in the MIMS cell with nitroblue tetrazolium as electron acceptor. Prior to the actual kinetic measurements, 3 μM H_2 was oxidized to approximately 500 nM H_2 over time and replenished to 3 μM H_2 several times, because we observed the enzyme needed to be activated to show a stable oxidation rate. Hereafter, the oxidation of 2.7 μM H_2 was followed over time (Fig. 2c). From this, a K_m value of 300 nM could be determined, which is higher than the values determined for whole cells and the membrane-associated Hyd-1h. We observed that the enzyme was stable over periods of several hours when H_2 was present at saturating concentrations. However, when H_2 had become depleted and the MIMS cell was again supplemented with 3 μM H_2, a significantly lower activity and lower affinity were observed. In the MIMS cell, submicromolar levels of O_2 are always present due to leakage. Only in the presence of the reducing agent dithiothreitol the oxygen problem could be overcome temporarily. Still, the activity of the isolated enzyme diminished over time in a buffered assay when H_2 had become

depleted. In conclusion, the isolated enzyme showed a lower affinity for H_2 compared with the membrane-associated enzyme, which could be explained by oxygen poisoning upon H_2 depletion, by the disconnection from the membrane or by a combination of both.

In order to determine the temperature optimum of the purified enzyme, the activity was measured spectrophotometrically in a range from 30 to 100 °C (Fig. 3a). A clear linear increase with every increment of 10 °C was observed from 40 to 80 °C. At the temperature optimum of 80 °C, the specific activity is approximately 7.5-fold higher compared with the specific activity at 30 °C. At 90 °C, roughly 30% of activity is lost in comparison to the optimum temperature, whereas at 100 °C all activity is lost. To determine the optimum pH of the hydrogenase, the activity was tested within a pH range of 4 to 10 (Fig. 3b). The acidity determines the charge of the amino acid residues and therefore has a profound effect on its folding and therefore its activity. A pH of 4 is too acidic for the enzyme to function, whereas a pH of 10 is too alkaline. A relative specific activity of 68 and 35% at respectively pH 7 and pH 9 was measured compared with the activity at the optimum pH of 8. To test the thermostability of the enzyme, the secondary structure and the activity were assessed at high temperatures. Remarkably, enzyme folding is recalcitrant to extremely high temperature, since the majority of the enzyme remains folded after at least 1 h at 95 °C as shown by circular dichroism measurements (Fig. 3c). Accordingly, the enzyme is able to largely retain its activity for a prolonged period at high temperature. Even at 80 °C the purified Hyd-1h from *M. fumariolicum* SolV retains a half-life stability of 30 min (Fig. 3d).

Discussion

In this study we show that the membrane-associated group 1h [NiFe] hydrogenase possesses a high apparent affinity for H_2, which enables the thermoacidophilic methanotroph *M. fumariolicum* SolV to oxidize subatmospheric H_2. Previous studies on atmospheric H_2 oxidation by soil bacteria had already revealed apparent kinetic parameters ($K_{m(app)} \sim$ 10–400 nM H_2) associated with this process [10, 12]. However, since these parameters were obtained in experiments with whole cells, it was unclear whether these low apparent affinity constants are attributable to intrinsic properties of the enzyme or to other cellular components, such as electron transport chain proteins [12]. We have shown that the membrane-associated Hyd-1h has a high apparent affinity ($K_{m(app)} = 140 \pm 10$ nM) for H_2, but that this affinity is lowered when the isolated enzyme is disconnected from the membrane ($K_m = 300$ nM). We therefore suggest that the membrane association of the group 1h

Fig. 3 Properties of the purified Hyd-1h at a range of conditions. a, b Relative specific activity (in % of the optimum activity) of the isolated hydrogenase (Hyd) and the control without enzyme (NC) within a temperature range of 30 to 100 °C (**a**) and within a pH range of 4 to 10 at 50 °C (**b**). **c** Circular dichroism spectrum from 200 to 260 nm measured after 1, 30, and 60 min incubation at 95 °C in 20 mM phosphate buffer (pH 7.0). **d** Residual activity (% of activity prior to heating) of the enzyme at 50 °C after incubation for 30 min at 70, 80, or 85 °C. Error bars indicate standard deviations ($n = 3$).
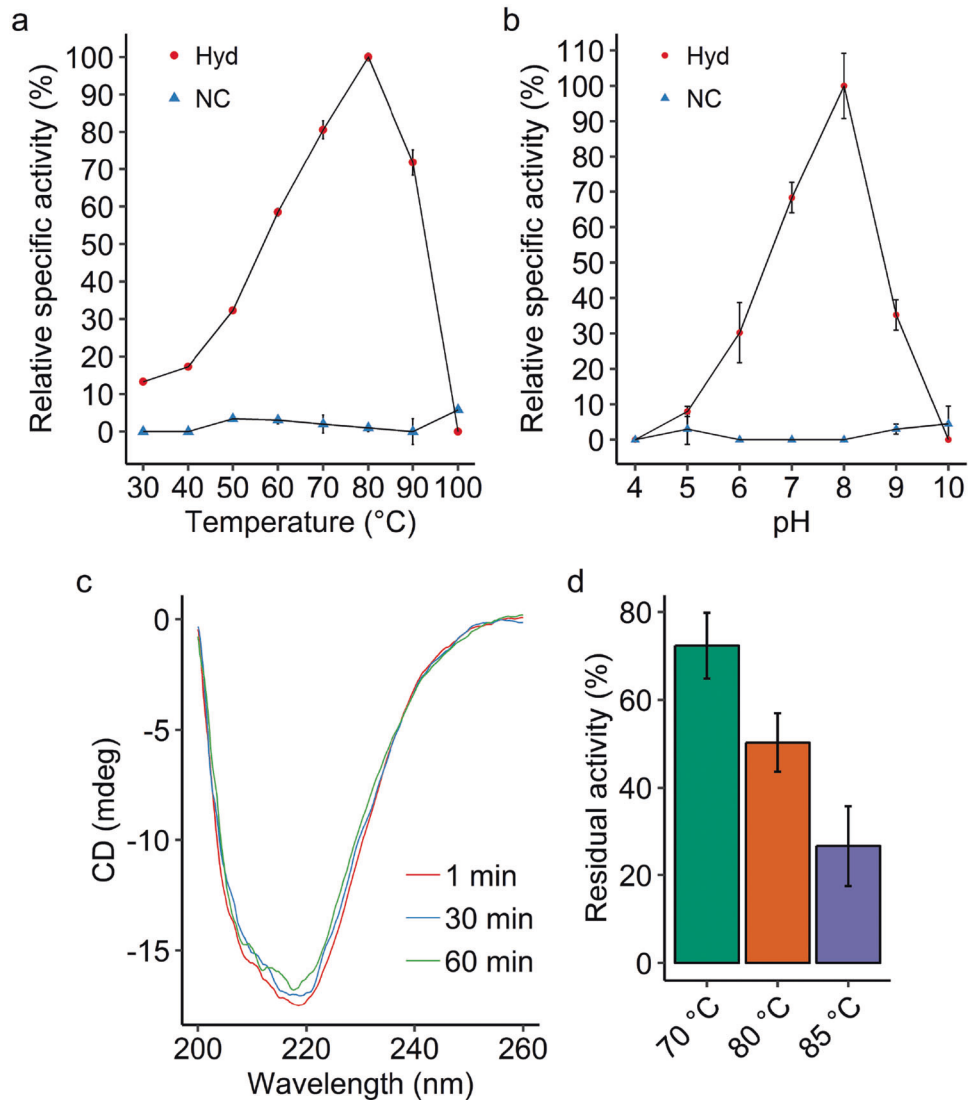
[NiFe] hydrogenase is pivotal for enzyme functioning and hence for atmospheric H_2 oxidation.

M. fumariolicum SolV is able to grow on CH_4 and H_2 concurrently as well as alternately [21, 22]. Moreover, growth on H_2 is possible by solely utilizing Hyd-1h, which is in contrast to other microorganisms harboring this enzyme, where it aids in cometabolism of H_2 for survival, not growth [15, 18, 22]. In *Mycobacterium smegmatis* mc^{2}155, cells expressing Hyd-1h consume H_2 with a maximum velocity of 2.5 pmol H_2 min^{-1} mg DW^{-1}, which is much slower than the 340 nmol H_2 min^{-1} mg DW^{-1} determined in this study [12]. Therefore, Hyd-1h of strain SolV seems to be tuned toward rapid oxidation and growth on H_2, whereas Actinobacteria and Chloroflexi use this enzyme to scavenge low concentrations of H_2 to persist during dormancy [12, 15, 18]. However, apparent kinetic parameters of strain SolV cells are similar to those of other microorganisms oxidizing atmospheric H_2. It was hypothesized that certain features in the respiratory chain or redox metabolism of *M. smegmatis* could contribute to the high affinity for H_2 [12]. Indeed, the affinity for H_2 is lowered when the enzyme is isolated and thus disconnected from the electron transport chain. Still, it is conceivable that we have not yet found the optimal in vitro conditions to reveal the true characteristics of the isolated enzyme. The apparent affinity of 190 ± 10 nM in cells of strain SolV significantly differs from the 0.6 μM measured by gas chromatography before, which could be attributed by limitations in gas–liquid mass transfer in the former study [22]. In general, H_2 is a key driver for microbial activity in geothermal areas and emitted at higher concentrations than the atmospheric H_2 concentration, although emissions can greatly vary spatiotemporally [6, 30, 38–40]. It is therefore conceivable that extremophilic methanotrophs such as strain SolV utilize Hyd-1h to rapidly oxidize H_2 as alternative energy source as well as persist on atmospheric H_2 in the natural environment.

This study describes the first purification of a putative high-affinity hydrogenase from an organism able to oxidize atmospheric H_2. Remarkably, Hyd-1h from *M. fumariolicum* SolV possesses distinct properties in comparison with the orthologue from *Ralstonia eutropha* H16, which was obtained by purification after homologous expression [14]. Because of its low-affinity Hyd-1h ($K_m = 3.6 \mu M$), this betaproteobacterium is unable to oxidize atmospheric H_2 [14]. Hyd-1h of *M. fumariolicum* SolV does not possess a membrane anchor but the enzyme is clearly associated with the membrane. This is in agreement with other bacteria harboring Hyd-1h, e.g., *Mycobacterium smegmatis* and *Pyrinomonas methylaliphatogenes* [12, 18]. This membrane association of Hyd-1h could be a determining factor in the high affinity for H_2, as in *R. eutropha* H16 the low-affinity enzyme was purified from the cytoplasm [14, 27]. Greening et al. have suggested a [2Fe2S] protein encoded in the Hyd-1h operon serves as intermediate redox partner. Indeed, these proteins are important in *Mycobacterium smegmatis*, but they are not conserved in all microorganisms that contain Hyd-1 and can oxidize atmospheric H_2 [41]. In addition, in the acidobacterium *Pyrinomonas methylaliphatogenes* the electron flow could be facilitated by hypothetical proteins in the Hyd-1h operon [18]. However, these homologous genes are not encoded in the genome of *M. fumariolicum* SolV. Moreover, in its Hyd-1h operon two hypothetical membrane proteins are encoded (MfumV2_0985-6) that are absent in Actinobacteria and Acidobacteria, but lack iron–sulfur clusters. The apparent affinity of the membrane-associated Hyd-1h ($K_{m(app)} = 140 nM$) is comparable to apparent affinities in cells of atmospheric H_2-oxidizing strains [10, 18, 27]. The isolated Hyd-1h in vitro, however, does not show a comparable high affinity for H_2 when disconnected from the membrane and is unable to oxidize subatmospheric H_2.

Purification of the enzyme allowed us to investigate the proposed characteristics (such as thermostability) of Hyd-1h [27]. Indeed, the enzyme is extremely thermostable, possessing a tenfold longer half-life time at 80 °C compared with the purified thermostable enzyme of *R. eutropha* H16 [14]. In addition, biophysical studies on the enzyme in UV-range revealed the enzyme to retain its folding at least for 1 h at 95 °C. The high thermostability could be explained by a combination of the proposed thermophilic origin of the enzyme and environmental pressure [27, 42]. Since *M. fumariolicum* SolV thrives in thermophilic habits instead of mesophilic habitats as *R. eutropha* H16 does, high temperature might be an environmental pressure for an even more heat-resistant enzyme. Studies on moderate temperature soils have shown cessation of atmospheric H_2 consumption above 40 °C [43]. However, this is likely due to heat sensitivity of the organism and not of the enzyme, since atmospheric H_2 oxidation at high temperatures was shown in Chloroflexi

and Acidobacteria strains [15, 18]. One of the reasons postulated for enzyme thermostability is the tight dimer packing of the enzyme [44]. The pH range in which the purified enzyme functions is similar to the purified protein of *R. eutropha* H16 at neutral range. However, the latter showed increased activity at pH > 10, outside of the physiological range [14]. In accordance with other studies, Hyd-1h of *M. fumariolicum* SolV remains active under ambient oxygen concentrations in the cell [22]. Furthermore, it could also be purified under aerobic conditions, while retaining catalytic activity. Interestingly, the enzyme from *R. eutropha* H16 was shown to be completely insensitive to oxygen. However, this was measured in the presence of high concentrations of H_2 that keep the enzyme in a reduced state. Group 1h [NiFe] hydrogenases are thought to possess specific mechanisms to cope with high O_2 levels, such as a narrow gas tunnel and a specific aspartate residue coordinating the proximal [4Fe4S] cluster [44]. However, we observed that in the absence of H_2, the isolated enzyme seems impeded by oxygen. Long-term storage was therefore done under anoxic conditions. Most hydrogenases are inhibited by the presence of O_2, therefore studying hydrogenases that show high tolerance to oxygen are interesting to study from a biotechnological perspective [45].

Utilization of both H_2 and CH_4 as energy source renders *M. fumariolicum* SolV metabolically flexible in ecosystems with fluctuations in H_2 and CH_4 emissions [22, 29, 38, 39]. In methanotrophs, Hyd-1h could therefore mitigate the emission of greenhouse gases from geothermal systems, especially in the presence of high O_2 concentrations. In addition, atmospheric H_2 controls the levels of atmospheric hydroxyl radicals and in turn the formation of methane [46]. We suggest strain SolV utilizes this enzyme to rapidly grow on H_2 and to scavenge atmospheric H_2 during persistence. The high affinity for H_2 is likely an ancient trait of the enzyme, used by soil-dwelling microorganisms in particular that persist on this ubiquitous atmospheric energy source [27]. We conclude that Hyd-1h has an important role in hostile methanotrophic systems for extremophilic methanotrophs to thrive and that at least a major part of atmospheric H_2 could be oxidized due to the membrane-associated Hyd-1h. Further work is needed to assess in which ecosystems microorganisms are actively oxidizing atmospheric H_2 and which hydrogenases are employed to catalyze this reaction.

Author contributions RAS, AP, SM, LJD, and HJMOdC designed research; RAS, AP, SM, CH, and AHvG performed research; RAS, AP, SM, LJD, and HJMOdC analyzed data; and RAS, AP, LJD, MSMJ, and HJMOdC wrote the paper.

Compliance with ethical standards

Conflict of interest The authors declare that they have no conflict of interest.

Publisher's note Springer Nature remains neutral with regard to jurisdictional claims in published maps and institutional affiliations.

References

1. Greening C, Biswas A, Carere CR, Jackson CJ, Taylor MC, Stott MB, et al. Genomic and metagenomic surveys of hydrogenase distribution indicate H$_2$ is a widely utilised energy source for microbial growth and survival. ISME J. 2016;10:761–77.

2. Lane N, Allen JF, Martin W. How did LUCA make a living? Chemiosmosis in the origin of life. Bioassays. 2010;32:271–80.

3. Lubitz W, Ogata H, Rüdiger O, Reijerse E. Hydrogenases. Chem Rev. 2014;114:4081–148.

4. Conrad R, Seiler W. Field measurements of hydrogen evolution by nitrogen-fixing legumes. Soil Biol Biochem. 1979;11:689–90.

5. Pester M, Brune A. Hydrogen is the central free intermediate during lignocellulose degradation by termite gut symbionts. ISME J. 2007;1:551–65.

6. Novelli PC. Molecular hydrogen in the troposphere: Global distribution and budget. J Geophys Res Atmos. 1999;104:30427–44.

7. Ehhalt DH, Rohrer F. The tropospheric cycle of H$_2$: a critical review. Tellus B. 2009;61:500–35.

8. Conrad R, Seiler W. Decomposition of atmospheric hydrogen by soil microorganisms and soil enzymes. Soil Biol Biochem. 1981;13:43–9.

9. Constant P, Poissant L, Villemur R. Isolation of *Streptomyces* sp. PCB7, the first microorganism demonstrating high-affinity uptake of tropospheric H$_2$. ISME J. 2008;2:1066–76.

10. Constant P, Chowdhury SP, Pratscher J, Conrad R. Streptomycetes contributing to atmospheric molecular hydrogen soil uptake are widespread and encode a putative high-affinity [NiFe]-hydrogenase. Environ Microbiol. 2010;12:821–9.

11. Constant P, Chowdhury SP, Hesse L, Pratscher J, Conrad R. Genome data mining and soil survey for the novel group 5 [NiFe]-hydrogenase to explore the diversity and ecological importance of presumptive high-affinity H$_2$-oxidizing bacteria. Appl Environ Microbiol. 2011;77:6027–35.

12. Greening C, Berney M, Hards K, Cook GM, Conrad R. A soil actinobacterium scavenges atmospheric H$_2$ using two membrane-associated, oxygen-dependent [NiFe] hydrogenases. Proc Natl Acad Sci USA. 2014;111:4257–61.

13. Myers MR, King GM. Isolation and characterization of *Acidobacterium ailaaui* sp. nov., a novel member of Acidobacteria subdivision 1, from a geothermally heated Hawaiian microbial mat. Int J Syst Evol Microbiol. 2016;66:5328–35.

14. Schäfer C, Friedrich B, Lenza O. Novel, oxygen-insensitive group 5 [NiFe]-hydrogenase in *Ralstonia eutropha*. Appl Environ Microbiol. 2013;79:5137–45.

15. Islam ZF, Cordero PRF, Feng J, Chen Y-J, Bay SK, Jirapanjawat T, et al. Two Chloroflexi classes independently evolved the ability to persist on atmospheric hydrogen and carbon monoxide. ISME J. 2019;13:1801–13.

16. Berney M, Cook GM. Unique flexibility in energy metabolism allows mycobacteria to combat starvation and hypoxia. PLoS ONE. 2010;5:e8614.

17. Greening C, Villas-Bôas SG, Robson JR, Berney M, Cook GM. The growth and survival of *Mycobacterium smegmatis* is enhanced by co-metabolism of atmospheric H$_2$. PLoS ONE. 2014;9:e103034.

18. Greening C, Carere CR, Rushton-Green R, Harold LK, Hards K, Taylor MC, et al. Persistence of the dominant soil phylum Acidobacteria by trace gas scavenging. Proc Natl Acad Sci USA. 2015;112:10497–502.

19. Meredith LK, Rao D, Bosak T, Klepac-Ceraj V, Tada KR, Hansel CM, et al. Consumption of atmospheric hydrogen during the life cycle of soil-dwelling actinobacteria. Environ Microbiol Rep. 2014;6:226–38.

20. Liot Q, Constant P. Breathing air to save energy - new insights into the ecophysiological role of high-affinity [NiFe]-hydrogenase in *Streptomyces avermitilis*. Microbiologyopen. 2016;5:47–59.

21. Pol A, Heijmans K, Harhangi HR, Tedesco D, Jetten MSM, Op den Camp HJM. Methanotrophy below pH 1 by a new Verrucomicrobia species. Nature. 2007;450:874–8.

22. Mohammadi S, Pol A, Van Alen TA, Jetten MS, Op Den Camp HJ. *Methylacidiphilum fumariolicum* SolV, a thermoacidophilic "Knallgas" methanotroph with both an oxygen-sensitive and -insensitive hydrogenase. ISME J. 2017;11:945–58.

23. Sharp CE, Smirnova AV, Graham JM, Stott MB, Khadka R, Moore TR, et al. Distribution and diversity of Verrucomicrobia methanotrophs in geothermal and acidic environments. Environ Microbiol. 2014;16:1867–78.

24. Bergmann GT, Bates ST, Eilers KG, Lauber CL, Caporaso JG, Walters WA, et al. The under-recognized dominance of Verrucomicrobia in soil bacterial communities. Soil Biol Biochem. 2011;43:1450–5.

25. Khadem AF, Pol A, Wieczorek A, Mohammadi SS, Francoijs KJ, Stunnenberg HG, et al. Autotrophic methanotrophy in Verrucomicrobia: *Methylacidiphilum fumariolicum* SolV uses the Calvin-Benson-Bassham cycle for carbon dioxide fixation. J Bacteriol. 2011;193:4438–46.

26. Pol A, Barends TRM, Dietl A, Khadem AF, Eygensteyn J, Jetten MSM, et al. Rare earth metals are essential for methanotrophic life in volcanic mudpots. Environ Microbiol. 2014;16:255–64.

27. Greening C, Constant P, Hards K, Morales SE, Oakeshott JG, Russell RJ, et al. Atmospheric hydrogen scavenging: from enzymes to ecosystems. Appl Environ Microbiol. 2015;81:1190–9.

28. Greening C, Cook GM. Integration of hydrogenase expression and hydrogen sensing in bacterial cell physiology. Curr Opin Microbiol. 2014;18:30–8.

29. Hanczár T, Csáki R, Bodrossy L, Murrell CJ, Kovács KL. Detection and localization of two hydrogenases in *Methylococcus capsulatus* (Bath) and their potential role in methane metabolism. Arch Microbiol. 2002;117:167–72.

30. Carere CR, Hards K, Houghton KM, Power JF, McDonald B, Collet C, et al. Mixotrophy drives niche expansion of verrucomicrobial methanotrophs. ISME J. 2017;11:2599–610.

31. Piché-Choquette S, Constant P. Molecular hydrogen, a neglected key driver of soil biogeochemical processes. Appl Environ Microbiol. 2019;85:e02418–18.

32. Wilhelm E, Battino R, Wilcock RJ. Low-pressure solubility of gases in liquid water. Chem Rev. 1977;77:219–62.

33. Versantvoort W, Pol A, Daumann LJ, Larrabee JA, Strayer AH, Jetten MSM, et al. Characterization of a novel cytochrome c_{GJ} as the electron acceptor of XoxF-MDH in the thermoacidophilic methanotroph *Methylacidiphilum fumariolicum* SolV. Biochim Biophys Acta. 2019;1867:595–603.

34. Britton HTS, Robinson AR. Universal buffer solutions and the dissociation constant of veronal. J Chem Soc. 1931;1931:1456–73.

35. Krogh A, Larsson B, von Heijne G, Sonnhammer ELL. Predicting transmembrane protein topology with a hidden Markov model: application to complete genomes. J Mol Biol. 2001;305:567–80.

36. Almagro Armenteros JJ, Tsirigos KD, Sønderby CK, Petersen TN, Winther O, Brunak S, et al. SignalP 5.0 improves signal peptide predictions using deep neural networks. Nat Biotechnol. 2019;37:420–3.

37. Cordero PRF, Grinter R, Hards K, Cryle MJ, Warr CG, Cook GM, et al. Two uptake hydrogenases differentially interact with the aerobic respiratory chain during mycobacterial growth and persistence. J Biol Chem. 2019. https://doi.org/10.1074/jbc.RA119.011076.

38. Power JF, Carere CR, Lee CK, Wakerley GLJ, Evans DW, Button M, et al. Microbial biogeography of 925 geothermal springs in New Zealand. Nat Commun. 2018;9:2876.

39. Spear JR, Walker JJ, McCollom TM, Pace NR. Hydrogen and bioenergetics in the Yellowstone geothermal ecosystem. Proc Natl Acad Sci USA. 2005;102:2555–60.

40. Meyer-Dombard DR, Shock EL, Amend JP. Archaeal and bacterial communities in geochemically diverse hot springs of Yellowstone National Park, USA. Geobiology. 2005;3:211–27.

41. Islam ZF, Cordero PRF, Greening C. Putative iron-sulfur proteins are required for hydrogen consumption and enhance survival of *Mycobacteria*. Front Microbiol. 2019;10:2479.

42. Scherr N, Nguyen L. *Mycobacterium* versus *Streptomyces*-we are different, we are the same. Curr Opin Microbiol. 2009; 12:699–707.

43. Chowdhury SP, Conrad R. Thermal deactivation of high-affinity H_2 uptake activity in soils. Soil Biol Biochem. 2010;42:1574–80.

44. Schäfer C, Bommer M, Hennig SE, Jeoung JH, Dobbek H, Lenz O. Structure of an actinobacterial-type [NiFe]-hydrogenase reveals insight into O_2-tolerant H_2 oxidation. Structure. 2016;24:285–92.

45. Vincent KA, Parkin A, Armstrong FA. Investigating and exploiting the electrocatalytic properties of hydrogenases. Chem Rev. 2007;107:4366–413.

46. Holmes CD, Prather MJ, Søvde OA, Myrhe G. Future methane, hydroxyl, and their uncertainties: key climate and emissions parameters for future predictions. Atmos Chem Phys. 2013;13:285–302.